

Analysis of the Mechanosensor Channel Functionality of TACAN

Yiming Niu¹, Xiao Tao^{1,4}, George Vaisey¹, Paul Dominic B. Olinares², Hanan Alwaseem³, Brian T. Chait² and Roderick MacKinnon^{1,4}

¹Laboratory of Molecular Neurobiology and Biophysics, ²Laboratory of Mass Spectrometry and Gaseous Ion Chemistry, ³Proteomics Resource Center, Rockefeller University, ⁴Howard Hughes Medical Institute, 1230 York Avenue, New York, NY 10065

Abstract

Mechanosensitive ion channels mediate transmembrane ion currents activated by mechanical forces. A mechanosensitive ion channel called TACAN was recently reported. We began to study TACAN with the intent to understand how it senses mechanical forces and functions as an ion channel. Using cellular patch-recording methods we failed to identify mechanosensitive ion channel activity. Using membrane reconstitution methods we found that TACAN, at high protein concentrations, produces non-selective, heterogeneous conduction levels that are not mechanosensitive and are most consistent with disruptions of the lipid bilayer. We determined the structure of TACAN using single particle cryo-EM and observe that it forms a symmetrical dimeric transmembrane protein. Each protomer contains an intracellular-facing cleft with a coenzyme-A co-factor, confirmed by mass spectrometry. The TACAN protomers are related in 3-dimensional structure to a fatty acid elongase, ELOVL. Whilst its physiological function remains unclear, we anticipate that TACAN is not a mechanosensitive ion channel.

INTRODUCTION

Numerous mechanosensitive ion channels (MSCs) have been discovered and characterized (Kefauver et al., 2020). By enabling mechanical forces to open conductive pores across the plasma membrane, MSCs mediate osmoregulation, cell and organ growth, blood pressure regulation, touch and hearing. Recently, a new MSC in mammals called TACAN was reported and proposed to mediate mechanical pain (Beaulieu-Laroche et al., 2020). Our laboratory studies the biophysical mechanisms by which MSCs transduce mechanical forces and conduct ions across membranes. We thus set out to study TACAN and report our findings here.

RESULTS

Functional analysis in cells and reconstituted membranes

We sought to reproduce the mechanically evoked currents reported when TACAN is expressed in cells (Beaulieu-Laroche et al., 2020). Using CHO cells, similar to those used in the original study, we did not observe pressure-evoked currents in excised membrane patches (Figure 1A, B). Background channels that were not sensitive to the pressure steps were observed in CHO cells expressing either TACAN or the M2 muscarinic receptor as a control. Similarly, TACAN expressed in a Piezo1 knockout HEK cell line did not elicit pressure-activated channels (Figure 1C, D). Purified TACAN protein reconstituted into giant unilamellar vesicles (GUVs) of soy L- α -phosphatidylcholine (soy-PC) also did not yield pressure-activated channels in membrane patches isolated from the GUVs (Figure 1E).

When TACAN was expressed, purified and reconstituted into both GUVs and planar lipid bilayers at high protein-to-lipid ratios ($\geq 1:100$, m:m) transient currents were observed, as shown (Figure 2). These currents were (i) not sensitive to pressure applied to patches isolated from the GUVs (Figure 1E), (ii) heterogeneous in amplitude (Figure 2A, B and D) and (iii) non-selective except for weak size selectivity (Figure 2C, F). These properties resemble no aspects of currents from known ion channels but are most consistent with TACAN rendering the membrane transiently leaky when reconstituted at high protein concentrations.

Structural analysis of TACAN

Alongside the functional characterization we analyzed the structure of TACAN determined at 3.5 Å resolution using single particle cryo-EM. Details of the structure determination are given in Methods and Table 1. TACAN is an α -helical transmembrane protein that forms a symmetric dimer (Figure 3A). The orientation of the protein with respect to the

cytoplasm is unknown, however, the charge distribution on TACAN (von Heijne, 1986) as well as the possible presence of an enzyme active site exposed to the cytoplasm (discussed below), suggest the orientation shown (Figure 3B). Each protomer consists of 6 transmembrane (TM) helices (S1-S6), which form a barrel surrounding a tunnel open to the cytoplasm (Figure 3C). Non-continuous density was observed inside the tunnel, suggesting the presence of a small, non-protein molecule (Figure 3 - figure supplement 3B). The two protomers of TACAN dimer bury an extensive surface area of 3049 Å², mediated through the TM domain as well as two long N-terminal helices that form a coiled coil (Figure 3A, Figure 3 - figure supplement 3A).

The DALI 3-dimensional structure comparison server (Holm and Rosenstrom, 2010) identified a homologous protein called ELOVL7, a long-chain fatty acid (FA) elongase (Figure 4). This enzyme catalyzes the first step in the FA elongation cycle by transferring an acetyl group from malonyl-CoA onto long chain FA-CoA (Naganuma et al., 2011). As shown in Figure 4A, the TM domain in TACAN is indeed similar to ELOVL7. The tunnel in ELOVL7 is lined by catalytically important histidine residues and contains a covalently linked eicosanoyl-CoA molecule (Figure 4B, C). TACAN conserves 2 of the 4 histidine residues (Figure 4B, D). To determine the identity of the small molecule implied by the broken density in the tunnel of TACAN (Figure 4E and Figure 3 - figure supplement 3B) we determined the structure of TACAN with His196 and His197 mutated to Alanine at 2.8 Å resolution (Figure 4 - figure supplement 1). The map showed clearer density consistent with a coenzyme-A molecule (CoASH) (Figure 4F). Native mass spectrometry (nMS) was used to confirm the identity as CoASH (Figure 5). As shown in Figure 5B, the purified TACAN^{H196A H197A} sample contains a mixture of the 83,237 Da, +767 Da, and +1,535 Da mass species, corresponding to an apo form, one and two CoASH bound forms, respectively. After incubation with CoASH, some fraction of the apo form shifts to one and two CoASH bound forms. Additionally, the +767 Da and +1,535 Da species are replaced by +795 Da and +1,591 Da or +811 Da and +1,622 Da species after incubation with the two CoASH analogues S-ethyl-CoA or Acetyl-CoA, corresponding to the CoASH analogue bound forms. In the purified TACAN^{WT} sample, the apo form is dominant and incubation with S-ethyl-CoA shifts it to one and two analogue bound forms (Figure 5A). Together, these data are consistent with our cryo-EM results and indicate that TACAN is co-purified with endogenous coenzyme-A.

It is noteworthy that CoASH binds with different conformations in TACAN from ELOVL7 (Figure 5 - figure supplement 1A, B). In addition, no enzymatic activity was observed for TACAN using a free-CoA detection assay (details see Methods) which demonstrated robust activity for

ELOVL7 ([Figure 5 - figure supplement 1C](#)), thus TACAN does not appear to catalyze the same reaction as ELOVL7. If TACAN is a coenzyme-A-dependent enzyme, its substrate is unknown.

Discussion

We undertook this study to understand how TACAN functions as an MSC, but have been unable to replicate evidence of MSC activity. We observe no channel activity in the plasma membrane of cells expressing TACAN and the non-selective, heterogeneous-in-amplitude currents (without mechanosensitive properties) that we observe when we reconstitute TACAN at high protein concentrations are not consistent with other native biological channels that we have studied. Structurally, TACAN is related to coenzyme-A-dependent fatty acid elongases, however, without further data we cannot conclude that TACAN itself functions as an enzyme. It also remains to be determined which membranes in a cell express TACAN. Previous studies suggested that TACAN is a nuclear envelope protein that participates in lipid metabolism (Batrakou et al., 2015; Byerly et al., 2010; Haakonsson et al., 2013; Lee et al., 2005; Rosell et al., 2014). Another study showed that adipocyte-specific TACAN knockout mice exhibit a lipodystrophy syndrome similar to human familial partial lipodystrophy FPLD2 (Czapiewski et al., 2021). In conclusion, we do not find evidence that TACAN is a mechanosensitive ion channel.

MATERIALS AND METHODS

Key resources table

Reagent type (species) or resource	Designation	Source or reference	Identifiers
Gene (Mus musculus TACAN)	<i>M. musculus</i> TACAN	synthetic	Synthesized at GeneWiz.
Gene (Homo sapiens TACAN)	<i>H. sapiens</i> TACAN	synthetic	Synthesized at GeneWiz.
Gene (Homo sapiens ELOVL7)	<i>H. sapiens</i> ELOVL7	synthetic	Synthesized at GeneWiz.
Strain, strain background (Escherichia coli)	DH10Bac	ThermoFisher	10361012
Recombinant DNA reagent	TACAN-eGFP BacMam	This study	
Recombinant DNA reagent	ELOVL7-eGFP BacMam	This study	
Recombinant DNA reagent	Halo-M2R-eGFP BacMam	This study	
Cell line (Spodoptera frugiperda)	Sf9	ATCC	Cat# CRL-1711
Cell line (Chinese hamster)	CHO-K1	ATCC	Cat# CRL-9618
Cell line (Homo sapiens)	HEK293S GnTI ⁻	ATCC	Cat# CRL-3022

Cell line (Homo sapiens)	Piezo1 knockout HEK293T	https://digitalcommons.rockefeller.edu/cgi/viewcontent.cgi?article=1422&context=student_theses_and_dissertations	
Chemical compound, drug	SF-900 II SFM medium	GIBCO	Cat# 11330-032
Chemical compound, drug	L-Glutamine (100x)	GIBCO	Cat# 25030-081
Chemical compound, drug	Pen Strep	GIBCO	Cat# 15140-122
Chemical compound, drug	Grace's insect medium	GIBCO	Cat# 11605-094
Chemical compound, drug	Freestyle 293 medium	GIBCO	Cat# 12338-018
Chemical compound, drug	DMEM/F-12 medium	GIBCO	Cat# 11605-094
Chemical compound, drug	DMEM	GIBCO	Cat# 11965-118
Chemical compound, drug	Fetal bovine serum	GIBCO	Cat# 16000-044
Chemical compound, drug	Cellfectin II reagent	Invitrogen	Cat# 10362100
Chemical compound, drug	FuGENE HD transfection reagent	Promega	E2312
Chemical compound, drug	Cholesteryl hemisuccinate (CHS)	Anatrace	CH210
Chemical compound, drug	n-Decyl- β -D-Maltopyranoside (DM)	Anatrace	D322S
Chemical compound, drug	Lauryl Maltose Neopentyl Glycol (LMNG)	Anatrace	Cat# NG310

Chemical compound, drug	Digitonin	Millipore Sigma	Cat# 300410
Chemical compound, drug	Coenzyme A trilithium salt (CoASH)	Sigma-Aldrich	C3019
Chemical compound, drug	Acetyl coenzyme A sodium salt (Acetyl-CoA)	Sigma-Aldrich	A2056
Chemical compound, drug	S-Ethyl-coenzyme A Sodium salt (S-Ethyl-CoA)	Jena-Biosciences	NU-1168
Chemical compound, drug	Malonyl coenzyme A lithium salt (Malonyl-CoA)	Sigma-Aldrich	M4263
Chemical compound, drug	Stearoyl coenzyme A lithium salt (Stearoyl-CoA)	Sigma-Aldrich	
Chemical compound, drug	(1H, 1H, 2H, 2H-Perfluorooctyl)phosphocholine (FFC8)	Anatrace	F300F
Commercial assay or kit	CNBr-activated Sepharose beads	GE Healthcare	Cat# 17-0430-01
Commercial assay or kit	Superdex 200 Increase 10/300 GL	GE Healthcare Life Sciences	28990944
Commercial assay or kit	R1.2/1.3 400 mesh Au holey carbon grids	Quantifoil	1210627
Commercial assay or kit	Coenzyme A (CoA) Assay Kit	Sigma-Aldrich	MAK034
Software, algorithm	RELION 3.0	https://doi.org/10.7554/eLife.42166.001	http://www2.mrc-lmb.cam.ac.uk/relion

Software, algorithm	RELION 3.1	https://doi.org/10.1101/798066	http://www2.mrc-lmb.cam.ac.uk/relion
Software, algorithm	MotionCor2	https://doi.org/10.1038/nmeth.4193	http://msg.ucsf.edu/em/software/motioncor2.html
Software, algorithm	Gctf 1.0.6	https://doi.org/10.1016/j.jsb.2015.11.003	https://www.mrc-lmb.cam.ac.uk/kzhang/Gctf/
Software, algorithm	CtfFind4.1.8	https://doi.org/10.1016/j.jsb.2015.08.008	http://grigoriefflab.janelia.org/ctffi4
Software, algorithm	CryoSPARC 2.9.0	https://doi.org/10.7554/eLife.46057.001	https://cryosparc.com/
Software, algorithm	COOT	https://doi.org/10.1107/S0907444910007493	http://www2.mrc-lmb.cam.ac.uk/personal/pemsley/coot
Software, algorithm	PHENIX	https://doi.org/10.1107/S0907444909052925	https://www.phenix-online.org

Software, algorithm	Adobe Photoshop version 16.0.0 (for figure preparation)	Adobe Systems, Inc.	
Software, algorithm	GraphPad Prism version 8.0	GraphPad Software	
Software, algorithm	MacPyMOL: PyMOL v2.0 Enhanced for Mac OS X	Schrodinger LLC	https://pymol.org/edu/?q=educational/
Software, algorithm	Chimera	https://doi.org/10.1002/jcc.20084	https://www.cgl.ucsf.edu/chimera/download.html
Software, algorithm	Serial EM	https://doi.org/10.1016/j.jsb.2005.07.007	http://bio3d.colorado.edu/SerialEM
Software, algorithm	pClamp	Axon Instruments, Inc	
Software, algorithm	Thermo Xcalibur Qual Browser (v. 4.2.47)	ThermoFisher Scientific	
Software, algorithm	UniDec v. 4.2.0	Marty et al., 2015; Reid et al., 2018	https://github.com/michaelmarty/UniDec/releases

Protein expression and purification

H. sapiens or *M. musculus* full-length TACAN (residues 1-343) were cloned into pEG BacMam (Goehring et al., 2014). The C-terminus of the TACAN construct contains a PreScission protease cleavage site and an enhanced green fluorescent protein (eGFP) for purification (TACAN-eGFP). Briefly, bacmid carrying TACAN was generated by transforming *E. coli* DH10Bac cells with the corresponding pEG BacMam construct according to the manufacturer's instructions (Bac-to-Bac; Invitrogen). Baculoviruses were produced by transfecting *Spodoptera frugiperda* Sf9 cells with the bacmid using Cellfectin II (Invitrogen). Baculoviruses, after two rounds of amplifications, were used for cell transduction. HEK293S GnTI⁻ cells (ATCC, CRL-3022) grown in suspension at a density of $\sim 3 \times 10^6$ cells/mL were transduced with P3 BacMam virus of TACAN-eGFP, and inoculated at 37°C. 8-12 hrs post-transduction, 10 mM sodium butyrate was added to the culture and cells were further inoculated for 40-48 hr at 30°C. Cells were then harvested by centrifugation, frozen in liquid N₂, and stored at -80°C until needed.

Frozen cells (from 1 L cell cultures) were resuspended in 200 mL hypotonic lysis buffer containing 50 mM Tris-HCl pH 8.0, 3 mM Dithiothreitol (DTT), 1 mM Ethylenediaminetetraacetic acid (EDTA), 0.1 mg/mL DNase I and a protease inhibitor cocktail (1 mM PMSF, 0.1 mg/mL trypsin inhibitor, 1 µg/mL pepstatin, 1 µg/mL leupeptin, and 1 mM benzamidine) for 30 min and centrifuged at 37,500 g for 30 min. The pellets were then homogenized in 20 mM Tris-HCl pH 8.0, 300 mM NaCl, 0.1 mg/mL DNase-I, a protease inhibitor cocktail followed by addition of 10 mM lauryl maltose neopentyl glycol (LMNG), 2 mM cholesteryl hemisuccinate (CHS) (for cryo-EM samples) or 1% n-Decyl-β-D-Maltopyranoside (DM), 0.2% CHS (w/v) (for reconstitution and mass spectrometry samples) to solubilize for 2 hrs. The suspension was then centrifuged at 37,500 g for 30 min and the supernatant incubated with 5 mL GFP nanobody-coupled CNBr-activated Sepharose resin (GE Healthcare) for 2 hrs (Kubala et al., 2010). The resin was subsequently washed with 10 column volumes of wash buffer containing 20 mM HEPES pH 7.4, 250 mM NaCl, and 0.06% Digitonin (w/v) (for cryoEM samples) or 0.25% DM, 0.05% CHS (w/v) (for reconstitution and mass spectrometry samples). The washed resin was incubated overnight with PreScission protease at a protein to protease ratio of 40:1 (w:w) to cleave off GFP and release the protein from the resin. The protein was eluted with wash buffer, concentrated using an Amicon Ultra centrifugal filter (MWCO 100 kDa), and then injected onto a Superdex 200 increase 10/300 GL column (GE Healthcare) equilibrated with the wash buffer. Peak fractions corresponding to the TACAN dimer were pooled. For cryoEM study, the pooled fractions were

concentrated to 6–7 mg/mL using an Amicon Ultra centrifugal filter (MWCO 100 kDa). All the purification steps were carried out at 4°C.

H. sapiens full-length ELOVL7 (residues 1-281) was cloned into the same vector, expressed and purified with the same protocol as TACAN in DM/CHS. The final protein concentration was ~2 mg/mL.

Proteoliposome reconstitution

Dialysis-mediated reconstitution of *H. sapiens* TACAN and ELOVL7 into liposome was accomplished according to published protocols with minor modifications (Brohawn et al., 2012; Heginbotham et al., 1999; Long et al., 2007; Tao and MacKinnon, 2008; Wang et al., 2014). Briefly, 20 mg of soy L- α -phosphatidylcholine (soy-PC) was dissolved in 1 mL chloroform in a glass vial and dried to a thin film under argon, rehydrated in reconstitution buffer (10 mM HEPES pH 7.4, 450 mM NaCl and 2 mM DTT) to 20 mg/mL by rotating for 20 min at room temperature, followed by sonication with a bath sonicator until translucent. 1% DM was then added, and the lipid detergent mixture was rotated for 30 min and sonicated again until clear. Purified TACAN (~3 mg/mL) or ELOVL7 (~2 mg/mL) in DM/CHS and DM-solubilized lipids (20 mg/mL) were mixed at protein-to-lipid (w:w) ratios of 1:20, 1:50 and 1:100, incubated for 2 hrs, and then dialyzed against 4 L reconstitution buffer for 4 days with daily exchange at 4°C. Biobeads (Biorad) were added to the reconstitution buffer for the last 12 hours. The resulting proteoliposomes were flash frozen in liquid N₂ and stored at –80°C.

GUV formation

The dehydration/rehydration mediated blister formation technique was used for generation of GUVs as previously reported (Brohawn et al., 2014). In brief, an aliquot of reconstituted *H. sapiens* TACAN proteoliposome was thawed at room temperature and spotted onto the 14-mm glass coverslip inside a 35-mm glass bottomed Petri dish (Mattek; P35G-1.5–14-C) as 4 to 6 similar-sized drops. Spotted proteoliposomes were then dried under vacuum at 4°C for 6 hrs followed by rehydration with ~20 μ L reconstitution buffer. The rehydration was done by sitting the 35-mm Petri dish inside a 15-cm Petri dish lined with wet filter paper overnight at 4°C (~16 hrs). 3 mL bath solution (10 mM HEPES pH 7.4, 140 mM KCl, 1 mM MgCl₂) was then added to the 35-mm dish before recording. Blisters were visible after ~10 min and were competent to form high resistance seals for at least 2 hrs.

Cell culture and transfection for patch recordings

CHO-K1 cells (ATCC) and piezo-1 knockout HEK-293T cells (established in this lab) were used for electrophysiology experiments because they have low endogenous mechanosensitive currents (Brohawn et al., 2014; del Marmol, 2016).

Cells were cultured in DMEM-F12 (Gibco) (CHO cells) or DMEM (Gibco) (HEK-293T cells) supplemented with 10% FBS, 2 mM L-glutamine, 100 units/mL penicillin, and 100 µg/mL streptomycin. Cells were plated in 35-mm plastic dishes and grown to ~50-60% confluency at 37°C. Right before transfection, culture media was replaced by DMEM-F12 or DMEM with 10 % FBS and 2 mM L-glutamine. 1 µg of *H. sapiens* TACAN-eGFP or the M2 muscarinic receptor (Halo-M2R-eGFP) plasmid (previously established in this lab) was transfected into the cells using FugeneHD (Promega) following the manufacturer's protocol. Cells were transferred to 30°C after transfection and recordings were carried out 16-18 hrs post-transfection. Immediately before recording, media were replaced by the bath solution (10 mM HEPES pH 7.4, 140 mM KCl, 1 mM MgCl₂).

Excised inside-out patch recordings

Pipettes of borosilicate glass (Sutter Instruments; BF150-86-10) were pulled to ~2-6 MΩ resistance with a micropipette puller (Sutter Instruments; P-97) and polished with a microforge (Narishige; MF-83). Recordings were obtained with an Axopatch 200B amplifier (Molecular Devices) using excised inside-out patch techniques. Recordings were filtered at 1 kHz and digitized at 10 kHz (Digidata 1440A; Molecular Devices). Pressure application through patch pipettes was performed with a high-speed pressure clamp (ALA Scientific) controlled through the Clampex software. Pressure application velocity was set to the maximum rate of 8.3 mmHg/msec.

All recordings were performed at room temperature. Pipette and bath solutions were identical unless otherwise stated: 10 mM HEPES pH 7.4, 140 mM KCl and 1 mM MgCl₂ (~300 Osm/L). For experiments described in [Figure 2C](#), the 140 mM KCl in pipette solution was substituted by either 15 mM KCl plus 125 mM NMDG-Cl, or 15 mM KCl and 125 K-Gluconate to study the ion selectivity of channel-like currents of TACAN.

Planar lipid bilayer recordings

The bilayer experiments were performed as previously described with minor modifications (Ruta et al., 2003; Wang et al., 2014). A piece of polyethylene terephthalate transparency film separated the two chambers of a polyoxymethylene block, filled with symmetrical buffer containing 10 mM HEPES pH 7.4, 150 mM KCl unless otherwise stated. A

lipid mixture of DPhPC (1,2-diphytanoyl-sn-glycero-3-phosphocholine, Avanti, Cat# 850356): POPA (1-palmitoyl-2-oleoyl-sn-glycero-3-phosphate, Avanti, Cat# 840857) (3:1, w:w) dissolved in decane (20 mg/mL) was pre-painted over a ~100 μm hole on the transparency film. Voltage was controlled with an Axopatch 200B amplifier in whole-cell mode. The analog current signal was low-pass filtered at 1 kHz (Bessel) and digitized at 10 kHz with a Digidata 1550A digitizer (Molecular Devices). Digitized data were recorded on a computer using the software pClamp (Molecular Devices, Sunnyvale, CA). Experiments were performed at room temperature. For experiments in [Figure 2F](#), 10 mM HEPES pH 7.4, 150 mM K-Gluconate (top chamber) and 10 mM HEPES pH 7.4, 15 mM K-Gluconate, 135 mM NMDG-Gluconate (bottom chamber), or 10 mM HEPES pH 7.4, 150 mM NMDG-HCl (top chamber) and 10 mM HEPES pH 7.4, 15 mM NMDG-HCl, 135 mM NMDG-Gluconate (bottom chamber) were used to study the cation and anion selectivity of TACAN currents, respectively.

Cryo-EM sample preparation and data collection

For both the WT and His196Ala, His197Ala mutant of *M. musculus* TACAN, purified protein at a concentration of 6–7 mg/mL was mixed with 2.9 mM Fluorinated Fos-Choline-8 (FFC8) (Anatrace) immediately prior to grid preparation. 3.5 μL of the mixture was applied onto a glow-discharged Quantifoil R1.2/1.3 400 mesh Au grid (Quantifoil), blotted for 4 s at room temperature (RT) with a blotting force of 2-4 and humidity of 100%, and plunge-frozen in liquid ethane using a Vitrobot Mark IV (FEI).

Cryo-EM data were collected on a 300-kV Titan Krios electron microscope (Thermo Fisher Scientific) equipped with a K2 Summit (TACAN^{WT}), or a K3 Summit (TACAN^{H196A H197A}) direct electron detector and a GIF Quantum energy filter set to a slit width of 20 eV. Images were automatically collected using SerialEM in super-resolution mode. After binning over 2 x 2 pixels, the calibrated pixel size was 1.03 Å with a preset defocus range from 0.7 to 2.1 μm (TACAN^{WT}), or 0.515 Å with a preset defocus range from 0.8 to 2.2 μm (TACAN^{H196A H197A}), respectively. Each image was acquired as either a 10-s movie stack of 50 frames with a dose rate of 7.54 e⁻/Å²/s, resulting in a total dose of about 75.4 e⁻/Å² (TACAN^{WT}), or a 1.5-s movie stack of 38 frames with a dose rate of 37.7 e⁻/Å²/s, resulting in a total dose of about 56.6 e⁻/Å² (TACAN^{H196A H197A}).

Image processing

For TACAN^{WT}, the image processing workflow is illustrated in [Figure 3 - figure supplement 1D](#). A total of 2,071 super-resolution movie stacks were collected. Motion-correction,

two-fold binning to a pixel size of 1.03 Å, and dose weighting were performed using MotionCor2 (Zheng et al., 2017). Contrast transfer function (CTF) parameters were estimated with Gctf (Zhang, 2016). Micrographs with ice or ethane contamination and empty carbon were removed manually, resulting in 1,982 micrographs for further processing. A total of 583,766 particles were auto-picked using Relion 3.1 (Scheres, 2019; Scheres, 2012; Zivanov et al., 2018; Zivanov et al., 2020) and windowed into 256 × 256-pixel images. Reference-free 2D classification was performed to remove contaminants, yielding 383,719 particles. These particles were subjected to Ab-initio reconstruction in cryoSPARC-2.9.0 (Punjani et al., 2017), specifying four output classes. The best class with 245,031 particles was selected, then subjected to a resolution-based classification workflow similar to a previous study (Kang et al., 2020). In brief, 40 iterations of global search 3D classification (K=1) in Relion 3.1 with an angular sampling step of 7.5° was performed to determine the initial alignment parameters using the initial model generated from cryoSPARC. For each of the last five iterations of the global search, a K=6 multi-reference local angular search 3D classification was performed with an angular sampling step of 3.75° and a search range of 30°. The multi-reference models were generated using reconstruction at the last iteration from global search 3D classification low-pass filtered to 8, 15, 25, 35, 45, and 55 Å, respectively. The classes that showed obvious secondary structure features were selected and combined. Duplicated particles were removed, yielding 130,491 particles in total. These particles were subsequently subjected to Non-uniform refinement with C2 symmetry in cryoSPARC, which resulted in a map with a resolution of 4.5 Å. Iterative cycles of Non-uniform refinement in cryoSPARC with C2 symmetry and Bayesian polishing in Relion 3.1 with new training parameters were performed until no further improvement, resulting a 3.7 Å map. The refined particles were further cleaned-up with one round of Ab-initio reconstruction (K=4) in cryoSPARC and 110,090 particles remained. Finally, these particles were subjected to the Non-uniform refinement with C2 symmetry in cryoSPARC, which yielded the final map at 3.5 Å resolution.

For TACAN^{H196A H197A}, 10,541 super-resolution movie stacks were collected. Motion-correction, two-fold binning to a pixel size of 0.515 Å, and dose weighting were performed using MotionCor2 (Zheng et al., 2017). CTF parameters were estimated with CTFFind4 (Rohou and Grigorieff, 2015). Micrographs with ice or ethane contamination and empty carbon were removed manually, resulting in 9,600 micrographs for further processing. A total of 1,474,917 particles were auto-picked using Relion 3.1 and windowed into 400 × 400-pixel images, then binned two times and subjected to 2D classification, yielding 975,636 particles. The following image processing workflow is identical to TACAN^{WT} sample. Briefly, these particles were

subjected to Ab-initio reconstruction in cryoSPARC-2.9.0 (Punjani et al., 2017), specifying four output classes. The best class with 607,159 particles was selected, then subjected to the resolution-based classification, yielding 391,137 particles. Subsequent Non-uniform refinement with C2 symmetry in cryoSPARC was performed, resulting in a map with a resolution of 3.8 Å and the resolution was further improved to 3.3 Å by iterative Bayesian polishing and Non-uniform refinement cycles. Particles were further cleaned-up with one round of Ab-initio reconstruction with 155,946 particles remained. Finally, these particles were subjected to the Non-uniform refinement with C2 symmetry in cryoSPARC, which yielded the final map at 2.8 Å resolution.

The mask-corrected FSC curves were calculated in cryoSPARC 2.9.0, and reported resolutions were based on the 0.143 criterion. Local resolutions of the final maps were estimated by Relion 3.1 (Scheres, 2019; Zivanov et al., 2020). A summary of reconstructions is shown in Table 1 and Figure 3 - figure supplement 1E-F, Figure 3 - figure supplement 2A-B, Figure 4 - figure supplement 1A-E.

Model building and refinement

For TACAN^{WT}, the 3.5 Å resolution map was subjected to Buccaneer in the CCP-EM suite (Burnley et al., 2017; Wood et al., 2015) to generate the de novo model. This initial model was further improved using phenix.sequence_from_map in Phenix (Adams et al., 2010). Several iterative cycles of refinement using the phenix.real_space_refine with secondary structure and NCS restraints and manual adjustments in COOT yielded the final model for the TACAN^{WT} containing residues 9-250 and 262-335 (Adams et al., 2010; Emsley et al., 2010).

For TACAN^{H196A H197A}, model of TACAN^{WT} was placed into the 2.8 Å map using UCSF Chimera (Pettersen et al., 2004) and manually adjusted in COOT (Emsley et al., 2010) followed by iterative refinement cycles using the phenix.real_space_refine in Phenix with secondary structure and NCS restraints and manual adjustments in COOT. The final model for TACAN^{H196A H197A} contained residues 9-72, 76-250, and 262-335 as well as two CoASH molecules bound.

Refinement statistics are summarized in Table 1. Structural model validation was done using Phenix and MolProbity based on the FSC = 0.5 criterion (Chen et al., 2010). Figures were prepared using PyMOL (<https://pymol.org/2/>) and UCSF Chimera (Pettersen et al., 2004). Representative densities of TACAN^{WT} and TACAN^{H196A H197A} are shown in Figure 3 - figure supplement 2C and Figure 4 - figure supplement 1F, respectively.

Native mass spectrometry (nMS) analysis

The purified wild-type and mutant *M. musculus* TACAN samples were incubated with excess (0.7 – 0.9 mM) ligand (CoASH, S-ethyl-CoA or acetyl-CoA) for 1 hr on ice. The incubated samples were then buffer exchanged into 200 mM ammonium acetate, 0.002% LMNG (2 CMC) using a Zeba microspin desalting column with a 40 kDa MWCO (ThermoFisher Scientific). For nMS analysis, a 2 to 3 μ L aliquot of each buffer-exchanged sample was loaded into a gold-coated quartz capillary tip that was prepared in-house and then electrosprayed into an Exactive Plus with extended mass range (EMR) instrument (Thermo Fisher Scientific) using a modified static direct infusion nanospray source (Olinares and Chait, 2020). The MS parameters used include: spray voltage, 1.22 – 1.25 kV; capillary temperature, 125 – 200 °C; in-source dissociation, 125 – 150 V; S-lens RF level, 200; resolving power, 8,750 or 17,500 at m/z of 200; AGC target, 1×10^6 ; maximum injection time, 200 ms; number of microscans, 5; injection flatapole, 8 V; interflatapole, 7 V; bent flatapole, 5 V; high energy collision dissociation (HCD), 200 V; ultrahigh vacuum pressure, $6 - 7 \times 10^{-10}$ mbar; total number of scans, at least 100. The instrument was mass calibrated in positive EMR mode using cesium iodide.

For data processing, the acquired MS spectra were visualized using Thermo Xcalibur Qual Browser (v. 4.2.47). MS spectra deconvolution was performed either manually or with UniDec v. 4.2.0 (Marty et al., 2015; Reid et al., 2018). The UniDec parameters used included: m/z range, 1,500 – 5,000; mass range, 20,000 – 100,000 Da; peak shape function, Gaussian, and smooth charge state distribution, on.

From their primary sequences, the expected masses for the proteins are TACAN^{WT} monomer: 41,770 Da, TACAN^{WT} dimer: 83,539 Da, TACAN^{H196A H197A} monomer: 41,637 Da, and TACAN^{H196A H197A} dimer: 83,275 Da. Experimental masses were determined as the average mass \pm standard deviation (S.D.) across all the calculated mass values in the relevant peak series ($n \geq 5$ charge states) with typical S.D.s of ± 1 Da.

Enzymatic activity assay to measure coenzyme A releasing

Coenzyme A releasing activity was measured using a fluorescence-based coupled-enzyme assay (Sigma-Aldrich, Cat. MAK034) in a 96-well microplate (Costar) at 37°C. The reaction was monitored with an Infinite-M1000 spectrofluorometer (Tecan) with 535-nm excitation and 587-nm emission. The reconstituted proteoliposomes of ELOVL7 and TACAN at 1:50 protein-to-lipid ratio were used (10 μ g total protein), supplemented with 100 μ M malonyl-CoA (Sigma-Aldrich, Cat. M4263) and 50 μ M stearoyl-CoA (Sigma-Aldrich Cat. S0802). Reaction mixtures were incubated at 37°C for 0, 0.5, 1, 2, 4, 8, 24 and 48 hrs, frozen in liquid N₂,

and stored at -80°C. The mixtures were then centrifuged at 20,817 g for 10 min and supernatants were used to perform the enzymatic assay following the manufacturer's protocol.

Acknowledgement

We thank Mark Ebrahim, Johanna Sotiris and Honkit Ng at the Evelyn Gruss Lipper Cryo-EM Resource Center at Rockefeller University for assistance in data collection; Dr. Chia-Hsueh Lee (St. Jude Children's Research Hospital) for critical reading of the manuscript and suggestions for image analysis; Dr. Yixiao Zhang for advice and help on data collection; and members of the MacKinnon lab and Chen lab (Rockefeller University) for assistance. This work was supported in part by GM43949 (to R.M.), GM109824 and GM103314 (to B.T.C.). R.M. is an investigator in the Howard Hughes Medical Institute.

REFERNECES

- Adams, P.D., Afonine, P.V., Bunkóczi, G., Chen, V.B., Davis, I.W., Echols, N., Headd, J.J., Hung, L.-W., Kapral, G.J., and Grosse-Kunstleve, R.W. (2010). PHENIX: a comprehensive Python-based system for macromolecular structure solution. *Acta Crystallographica Section D: Biological Crystallography* 66, 213-221.
- Batrakou, D.G., de Las Heras, J.I., Czapiewski, R., Mouras, R., and Schirmer, E.C. (2015). TMEM120A and B: nuclear envelope transmembrane proteins important for adipocyte differentiation. *PLoS One* 10, e0127712.
- Beaulieu-Laroche, L., Christin, M., Donoghue, A., Agosti, F., Yousefpour, N., Petitjean, H., Davidova, A., Stanton, C., Khan, U., Dietz, C., *et al.* (2020). TACAN Is an Ion Channel Involved in Sensing Mechanical Pain. *Cell* 180, 956-967.e917.
- Brohawn, S.G., Del Mármol, J., and MacKinnon, R. (2012). Crystal structure of the human K2P TRAAK, a lipid-and mechano-sensitive K⁺ ion channel. *Science* 335, 436-441.
- Brohawn, S.G., Su, Z., and MacKinnon, R. (2014). Mechanosensitivity is mediated directly by the lipid membrane in TRAAK and TREK1 K⁺ channels. *Proceedings of the National Academy of Sciences* 111, 3614-3619.
- Burnley, T., Palmer, C.M., and Winn, M. (2017). Recent developments in the CCP-EM software suite. *Acta Crystallographica Section D: Structural Biology* 73, 469-477.
- Byerly, M.S., Simon, J., Cogburn, L.A., Le Bihan-Duval, E., Duclos, M.J., Aggrey, S.E., and Porter, T.E. (2010). Transcriptional profiling of hypothalamus during development of adiposity in genetically selected fat and lean chickens. *Physiological genomics* 42, 157-167.

Chen, V.B., Arendall, W.B., Headd, J.J., Keedy, D.A., Immormino, R.M., Kapral, G.J., Murray, L.W., Richardson, J.S., and Richardson, D.C. (2010). MolProbity: all-atom structure validation for macromolecular crystallography. *Acta Crystallographica Section D: Biological Crystallography* 66, 12-21.

Czapiewski, R., Batrakou, D.G., de las Heras, J.I., Carter, R.N., Sivakumar, A., Sliwinska, M., Dixon, C.R., Webb, S., Lattanzi, G., and Morton, N.M. (2021). Genomic loci mispositioning in Tmem120a knockout mice yields latent lipodystrophy. *bioRxiv*.

del Marmol, J.I. (2016). Molecular Basis of Mechanosensitivity.

Emsley, P., Lohkamp, B., Scott, W.G., and Cowtan, K. (2010). Features and development of Coot. *Acta Crystallographica Section D: Biological Crystallography* 66, 486-501.

Goehring, A., Lee, C.-H., Wang, K.H., Michel, J.C., Claxton, D.P., Bacongus, I., Althoff, T., Fischer, S., Garcia, K.C., and Gouaux, E. (2014). Screening and large-scale expression of membrane proteins in mammalian cells for structural studies. *Nature protocols* 9, 2574.

Haakonsson, A.K., Stahl Madsen, M., Nielsen, R., Sandelin, A., and Mandrup, S. (2013). Acute genome-wide effects of rosiglitazone on PPAR γ transcriptional networks in adipocytes. *Molecular endocrinology* 27, 1536-1549.

Heginbotham, L., LeMasurier, M., Kolmakova-Partensky, L., and Miller, C. (1999). Single *Streptomyces lividans* K⁺ channels: functional asymmetries and sidedness of proton activation. *The Journal of general physiology* 114, 551-560.

Heijne, G. (1986). The distribution of positively charged residues in bacterial inner membrane proteins correlates with the trans-membrane topology. *Embo j* 5, 3021-3027.

Holm, L., and Rosenstrom, P. (2010). Dali server: conservation mapping in 3D. *Nucleic Acids Res* 38, W545-549.

Kang, Y., Wu, J.-X., and Chen, L. (2020). Structure of voltage-modulated sodium-selective NALCN-FAM155A channel complex. *Nature Communications* 11, 6199.

Kefauver, J., Ward, A., and Patapoutian, A. (2020). Discoveries in structure and physiology of mechanically activated ion channels. *Nature* 587, 567-576.

Lee, Y., Nair, S., Rousseau, E., Allison, D., Page, G., Tataranni, P., Bogardus, C., and Permana, P. (2005). Microarray profiling of isolated abdominal subcutaneous adipocytes from obese vs non-obese Pima Indians: increased expression of inflammation-related genes. *Diabetologia* 48, 1776-1783.

Long, S.B., Tao, X., Campbell, E.B., and MacKinnon, R. (2007). Atomic structure of a voltage-dependent K⁺ channel in a lipid membrane-like environment. *Nature* 450, 376-382.

- Marty, M.T., Baldwin, A.J., Marklund, E.G., Hochberg, G.K., Benesch, J.L., and Robinson, C.V. (2015). Bayesian deconvolution of mass and ion mobility spectra: from binary interactions to polydisperse ensembles. *Analytical chemistry* 87, 4370-4376.
- Naganuma, T., Sato, Y., Sassa, T., Ohno, Y., and Kihara, A. (2011). Biochemical characterization of the very long-chain fatty acid elongase ELOVL7. *FEBS letters* 585, 3337-3341.
- Olinares, P.D.B., and Chait, B.T. (2020). Native mass spectrometry analysis of affinity-captured endogenous yeast RNA exosome complexes. In *The Eukaryotic RNA Exosome* (Springer), pp. 357-382.
- Pettersen, E.F., Goddard, T.D., Huang, C.C., Couch, G.S., Greenblatt, D.M., Meng, E.C., and Ferrin, T.E. (2004). UCSF Chimera—a visualization system for exploratory research and analysis. *Journal of computational chemistry* 25, 1605-1612.
- Punjani, A., Rubinstein, J.L., Fleet, D.J., and Brubaker, M.A. (2017). cryoSPARC: algorithms for rapid unsupervised cryo-EM structure determination. *Nature methods* 14, 290-296.
- Reid, D.J., Diesing, J.M., Miller, M.A., Perry, S.M., Wales, J.A., Montfort, W.R., and Marty, M.T. (2018). MetaUniDec: high-throughput deconvolution of native mass spectra. *Journal of the American Society for Mass Spectrometry* 30, 118-127.
- Rohou, A., and Grigorieff, N. (2015). CTFFIND4: Fast and accurate defocus estimation from electron micrographs. *Journal of structural biology* 192, 216-221.
- Rosell, M., Kaforou, M., Frontini, A., Okolo, A., Chan, Y.-W., Nikolopoulou, E., Millership, S., Fenech, M.E., MacIntyre, D., and Turner, J.O. (2014). Brown and white adipose tissues: intrinsic differences in gene expression and response to cold exposure in mice. *American Journal of Physiology-Endocrinology and Metabolism* 306, E945-E964.
- Ruta, V., Jiang, Y., Lee, A., Chen, J., and MacKinnon, R. (2003). Functional analysis of an archaeobacterial voltage-dependent K⁺ channel. *Nature* 422, 180-185.
- Scheres, S. (2019). Amyloid structure determination in RELION-3.1. *BioRxiv*, 823310.
- Scheres, S.H. (2012). RELION: implementation of a Bayesian approach to cryo-EM structure determination. *Journal of structural biology* 180, 519-530.
- Tao, X., and MacKinnon, R. (2008). Functional analysis of Kv1. 2 and paddle chimera Kv channels in planar lipid bilayers. *Journal of molecular biology* 382, 24-33.
- Wang, W., Whorton, M.R., and MacKinnon, R. (2014). Quantitative analysis of mammalian GIRK2 channel regulation by G proteins, the signaling lipid PIP2 and Na⁺ in a reconstituted system. *Elife* 3, e03671.

- Wood, C., Burnley, T., Patwardhan, A., Scheres, S., Topf, M., Roseman, A., and Winn, M. (2015). Collaborative computational project for electron cryo-microscopy. *Acta Crystallographica Section D: Biological Crystallography* 71, 123-126.
- Zhang, K. (2016). Gctf: Real-time CTF determination and correction. *Journal of structural biology* 193, 1-12.
- Zheng, S.Q., Palovcak, E., Armache, J.-P., Verba, K.A., Cheng, Y., and Agard, D.A. (2017). MotionCor2: anisotropic correction of beam-induced motion for improved cryo-electron microscopy. *Nature methods* 14, 331-332.
- Zivanov, J., Nakane, T., Forsberg, B.O., Kimanius, D., Hagen, W.J., Lindahl, E., and Scheres, S.H. (2018). New tools for automated high-resolution cryo-EM structure determination in RELION-3. *Elife* 7, e42166.
- Zivanov, J., Nakane, T., and Scheres, S.H. (2020). Estimation of high-order aberrations and anisotropic magnification from cryo-EM data sets in RELION-3.1. *IUCrJ* 7.

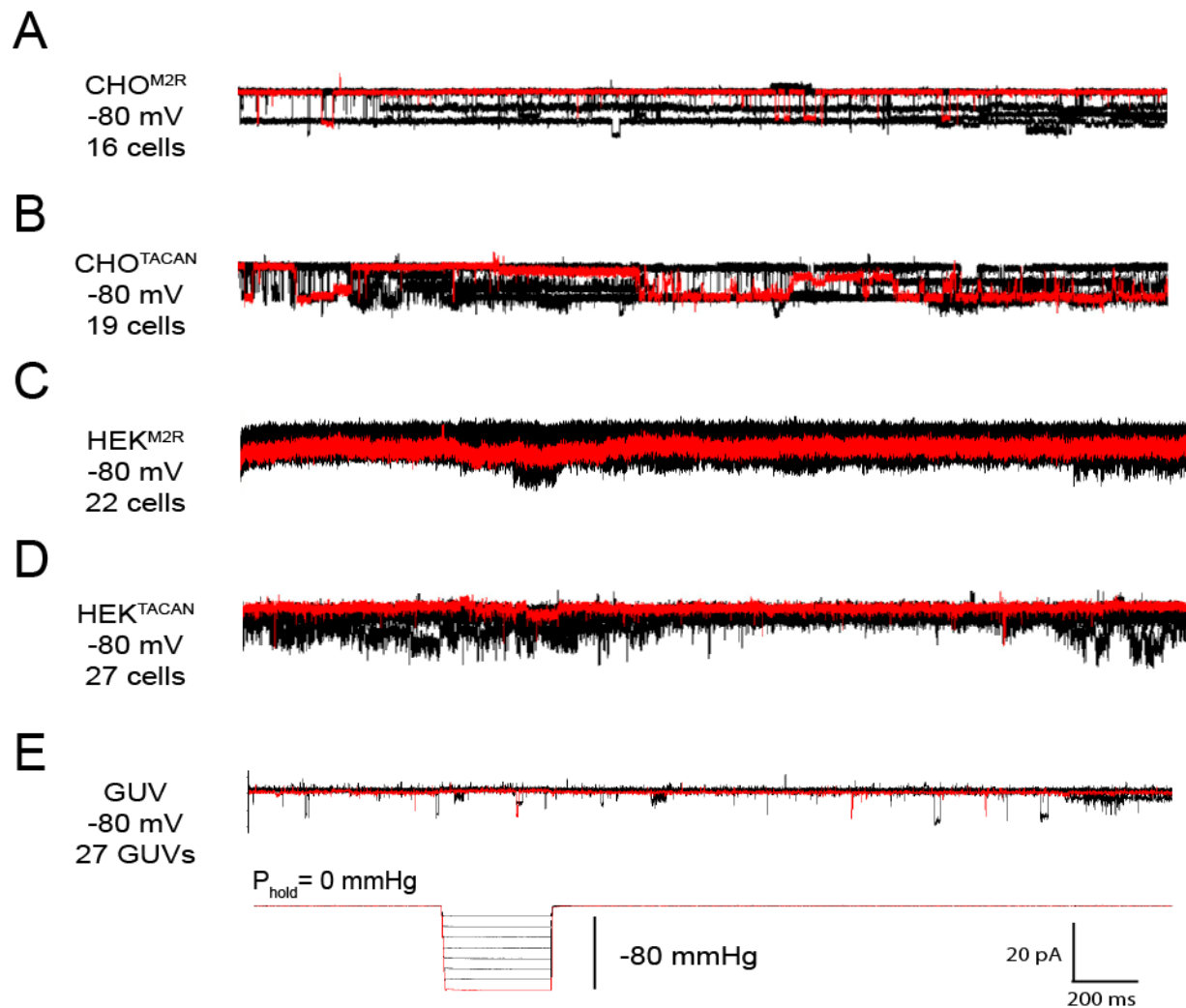


Figure 1. TACAN does not produce mechanically evoked currents.

(A-B) Representative excised inside-out patch recordings of M2 muscarinic receptor (M2R, A) and TACAN (B) transfected into CHO-K1 cells.

(C-D). Representative excised inside-out patch recordings of M2R (C) and TACAN (D) transfected into piezo-1 knockout HEK-293T cells.

(E) Representative excised inside-out patch recording of TACAN reconstituted in GUVs.

All recordings were performed with identical pipette and bath solution containing 10 mM HEPES pH 7.4, 140 mM KCl and 1 mM MgCl_2 (~300 Osm/L). Traces were obtained holding at -80 mV with a pressure pulse protocol shown at the bottom: 0 to -80 mmHg with 10 mmHg step. Traces colored in red represent the observed currents with -80 mmHg pressure pulse.

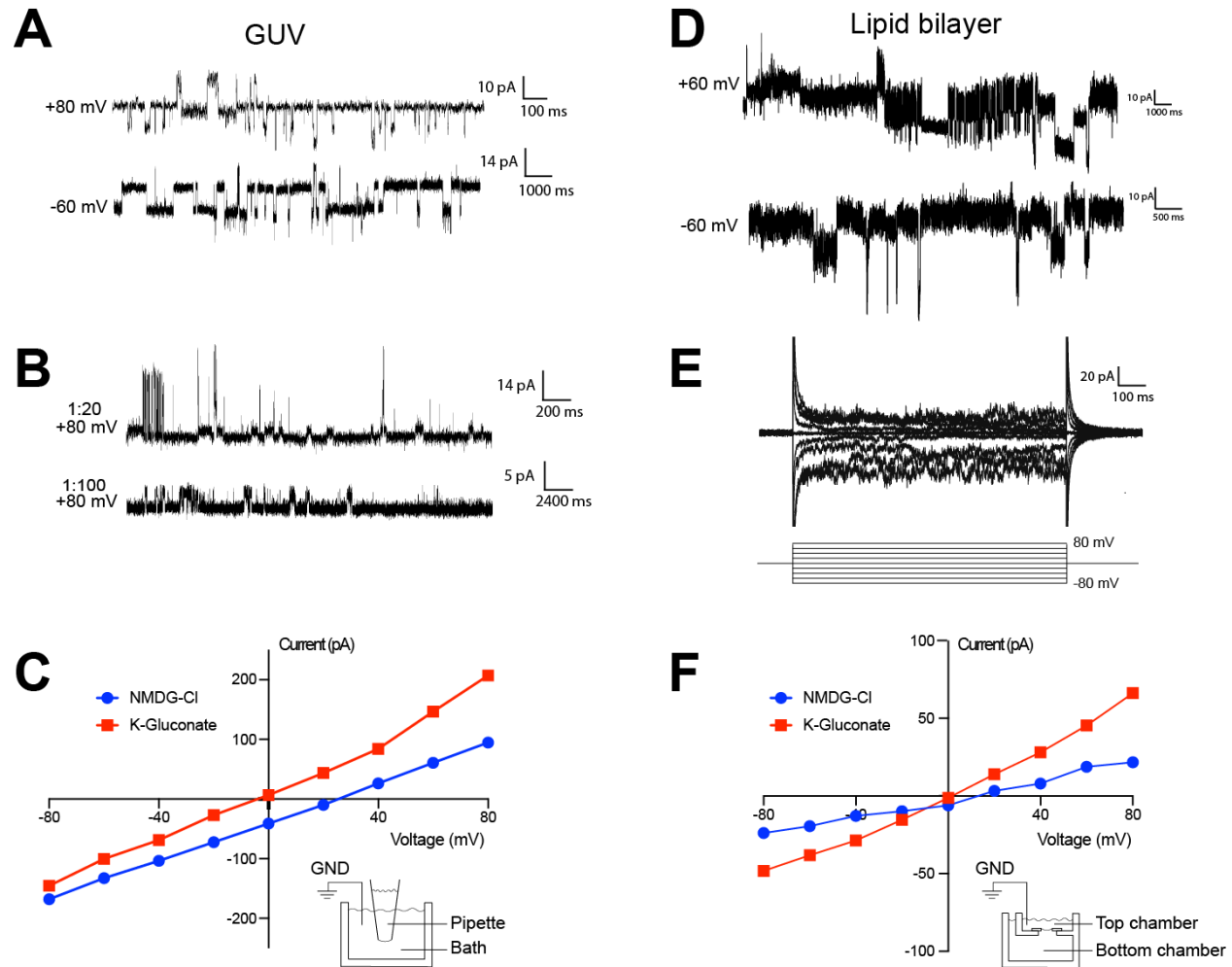


Figure 2. TACAN produces heterogeneous currents in reconstituted systems.

(A-B) Representative recordings of TACAN from excised GUV patches. Symmetrical buffers (10 mM HEPES pH 7.4, 140 mM KCl, 1 mM MgCl_2) were used in pipette and bath. (A) Traces of GUVs at 1:20 protein-to-lipid ratio (w/w) holding at +80 mV and -60 mV. (B) Traces of GUVs at 1:20 and 1:100 protein-to-lipid ratio (w/w) holding at +80 mV.

(C) Current-voltage relationships of TACAN in excised GUV patches recorded with a voltage family protocol from -80 to +80 mV in 20 mV increment. Asymmetric recording buffers were used to study the cation and anion selectivity. As shown in the cartoon, for the blue curve (NMDG-Cl), pipette contains 10 mM HEPES pH 7.4, 15 mM KCl plus 125 mM NMDG-Cl, 1 mM MgCl_2 and bath contains 10 mM HEPES pH 7.4, 140 mM KCl, 1 mM MgCl_2 ; For the red curve (K-Gluconate), pipette contains 10 mM HEPES pH 7.4, 15 mM KCl plus 125 mM K-Gluconate, 1 mM MgCl_2 and bath contains 10 mM HEPES pH 7.4, 140 mM KCl, 1 mM MgCl_2 .

(D-E) Representative traces of TACAN reconstituted in a lipid bilayer. Symmetrical buffers (10 mM HEPES pH 7.4, 150 mM KCl) were used in top and bottom chambers. (D) Traces holding at

+60 mV and -60 mV. (E) Trace recorded with a voltage family from -80 to +80 mV in 20 mV increment.

(F) Current-voltage relationships for bilayer recordings of TACAN in asymmetric ionic conditions. For the blue curve (NMDG-Cl), top chamber contains 10 mM HEPES pH 7.4, 150 mM K-Gluconate and bottom chamber contains 10 mM HEPES pH 7.4, 15 mM K-Gluconate plus 135 mM NMDG-Gluconate. For the red curve (K-Gluconate), top chamber contains 10 mM HEPES pH 7.4, 150 mM NMDG-HCl and bottom chamber contains 10 mM HEPES pH 7.4, 15 mM NMDG-HCl plus 135 mM NMDG-Gluconate. The bilayer setup is shown as a cartoon representation.

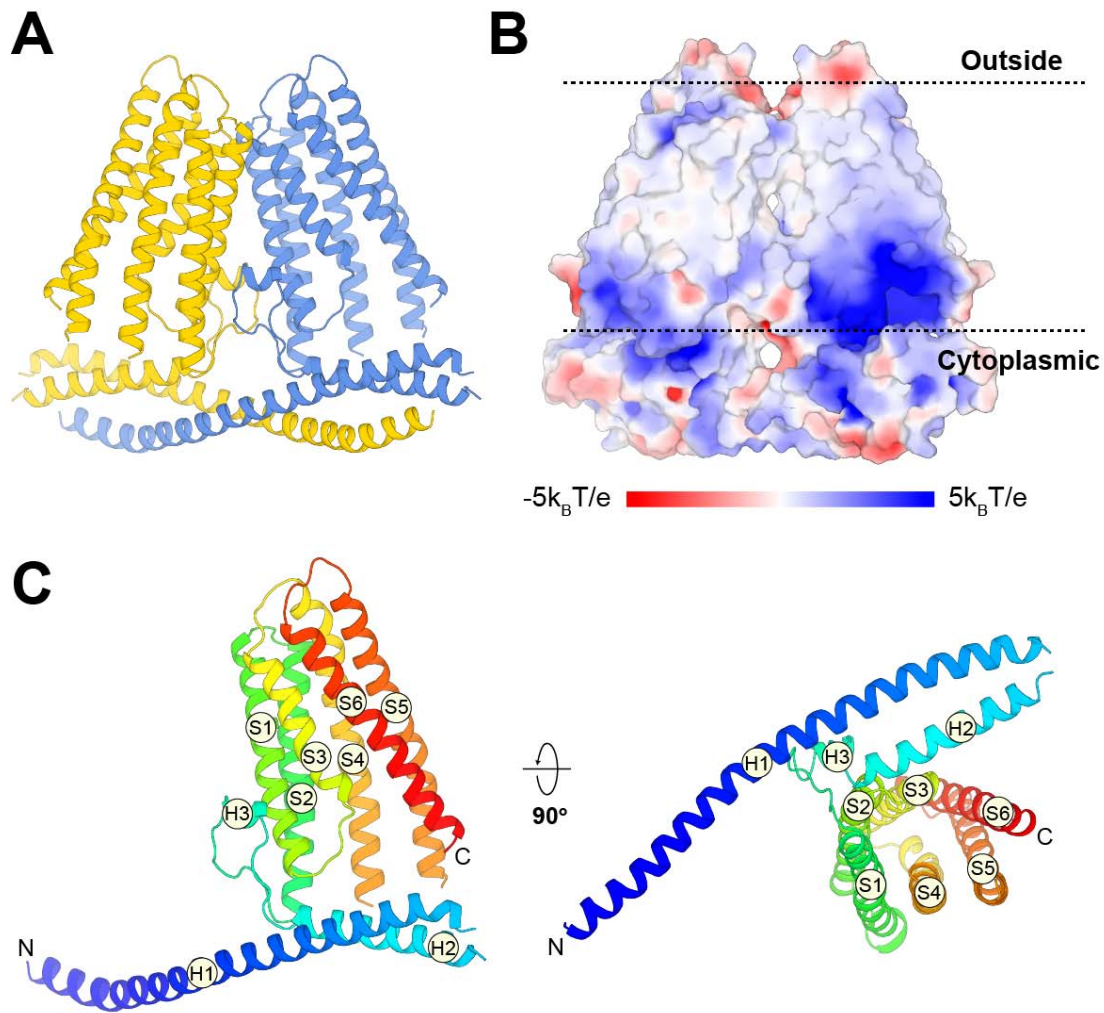


Figure 3. Overall structure of TACAN.

(A) Cartoon representation of the TACAN dimer with each protomer colored uniquely.

(B) Surface charge distribution and the possible orientation of TACAN, blue and red representing the positive and negative charges, respectively. The membrane is demarcated by dashed lines.

(C) Tertiary structure of TACAN protomer viewed from the side and the cytoplasmic side. The protein is colored rainbow from N-terminus (blue) to C-terminus (red). The six transmembrane helices (S1-S6), two horizontal helices (H1 and H2) as well as a short helix (H3) in between are labelled.

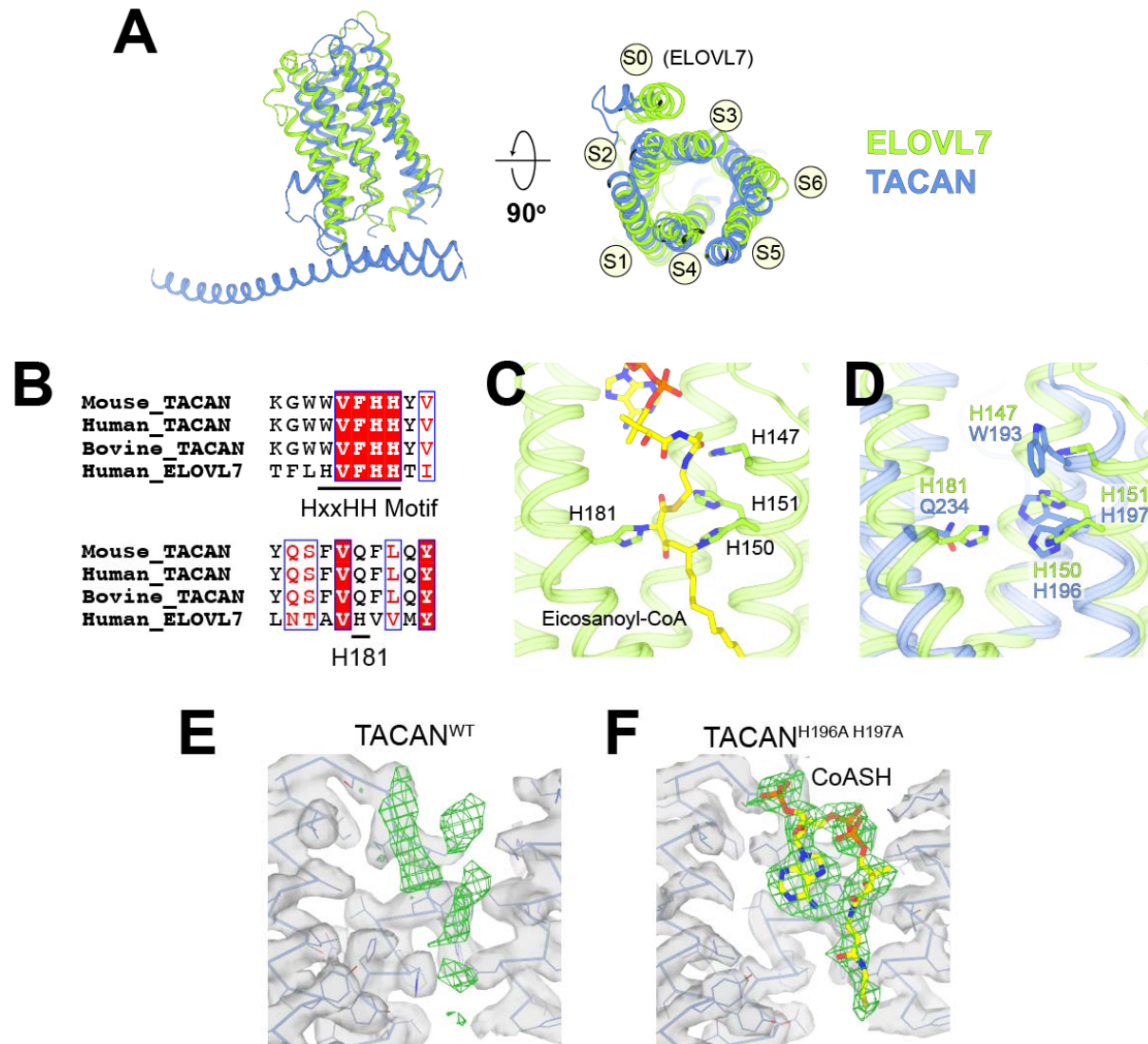


Figure 4. TACAN shares structural homology to the fatty acid elongase ELOVL7.

(A) Superposition between TACAN (blue) and ELOVL7 (green) protomers. Transmembrane helices are labeled to correspond with the topology of TACAN. The extra transmembrane helix in ELOVL7 is labeled as S0.

(B) Sequence alignment of TACAN from different species and human ELOVL7 with conserved residues highlighted. The catalytically important HxxHH motif (His147, His150 and His151) and His181 in ELOVL7 are underlined.

(C) Structure details of the interactions between the HxxHH motif, His181 (sidechains shown as sticks) and eicosanoyl-CoA (shown as sticks) in ELOVL7 (PDB: 6Y7F). His150 and His181 are covalently linked to eicosanoyl-CoA.

(D) Zoom-in view of the ELOVL7 (green) catalytic center with TACAN (blue) superimposed.

(E and F) The non-protein density (green mesh) in the narrow tunnel of wild-type (E) and His196Ala, His197Ala mutant of TACAN (F). Protein density is represented as transparent surface (gray) with protein shown as lines and ribbons. The two maps are shown at the same contour level. CoASH in mutant TACAN is shown as sticks and colored according to atom type.

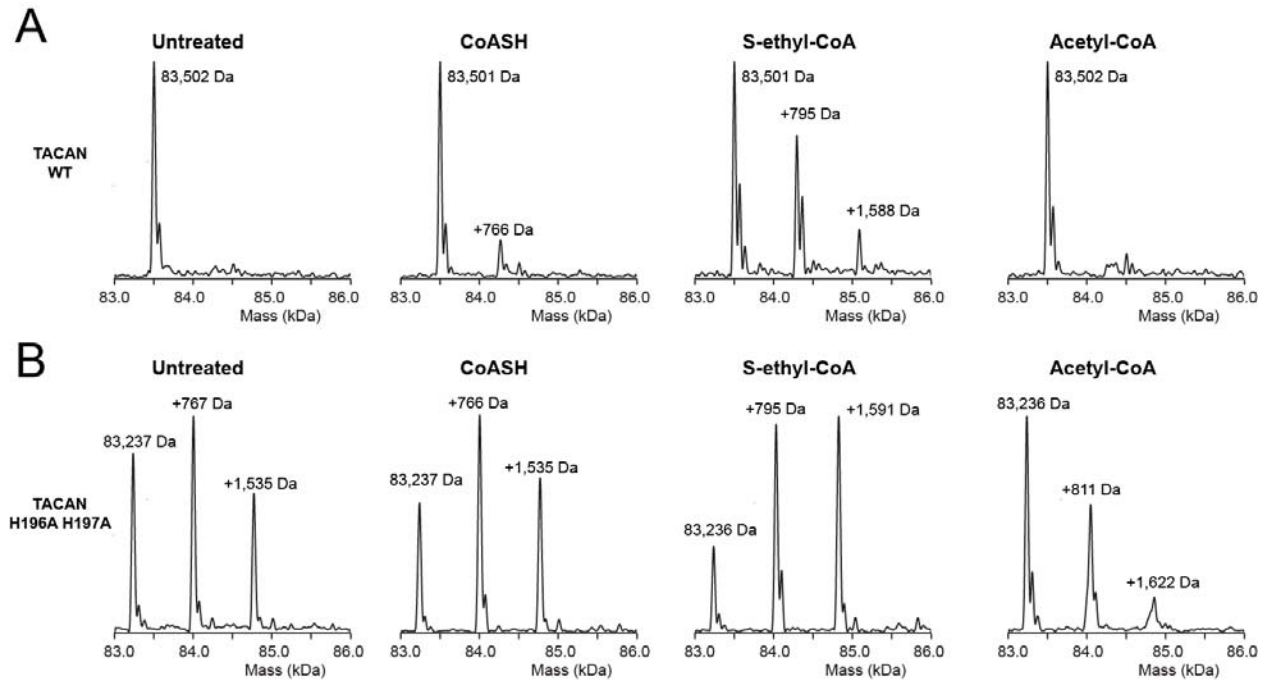


Figure 5. Mass spectrometry indicates the presence of coenzyme A in the mutant TACAN sample

(A and B) Mass species detected in purified wild-type (A) and His196Ala, His197Ala mutant (B) TACAN protein without treatment (“untreated”), or incubated with CoASH (MW = 767.5 Da), S-ethyl-CoA (MW = 795.6 Da) or Acetyl-CoA (MW = 809.6 Da).

Table 1. Cryo-EM data collection and refinement statistics, related to Figures 3 and 4.

	TACAN ^{WT}	TACAN ^{H196A H197A}
EMDB ID	EMD-24107	EMD-24108
PDB ID	7NOK	7NOL
Data collection		
Microscope	Titan Krios	
Detector	K2 summit	K3 summit
Voltage (kV)	300	
Pixel size (Å)	1.03	0.515
Total electron exposure (e ⁻ /Å ²)	75.4	56.6
Defocus range (µm)	0.7 to 2.1	0.8 to 2.2
Micrographs collected	2,017	10,541
Reconstruction		
Final particle images	110,090	155,946
Pixel size (Å)	1.03	1.03
Box size (pixels)	256	256
Resolution (Å) (FSC = 0.143)	3.5	2.8
Map Sharpening B-factor (Å ²)	-20	-3.4
Model composition		
Non-hydrogen atoms	5,156	5,272
Protein residues	626	626
Ligands	0	2
Metals	0	0
Refinement		
Model-to-map CC (mask)	0.77	0.80
Model-to-map CC (volume)	0.73	0.81
R.m.s deviations		
Bond length (Å)	0.003	0.003
Bond angles (°)	0.54	0.52
Validation		
MolProbity score	2.09	2.22
Clash score	7.86	9.10
Ramachandran plot		
Outliers (%)	0.0	0
Allowed (%)	0.98	1.95
Favored (%)	99.02	98.05
Rotamer outliers (%)	7.46	9.23
C-beta deviations (%)	0	0

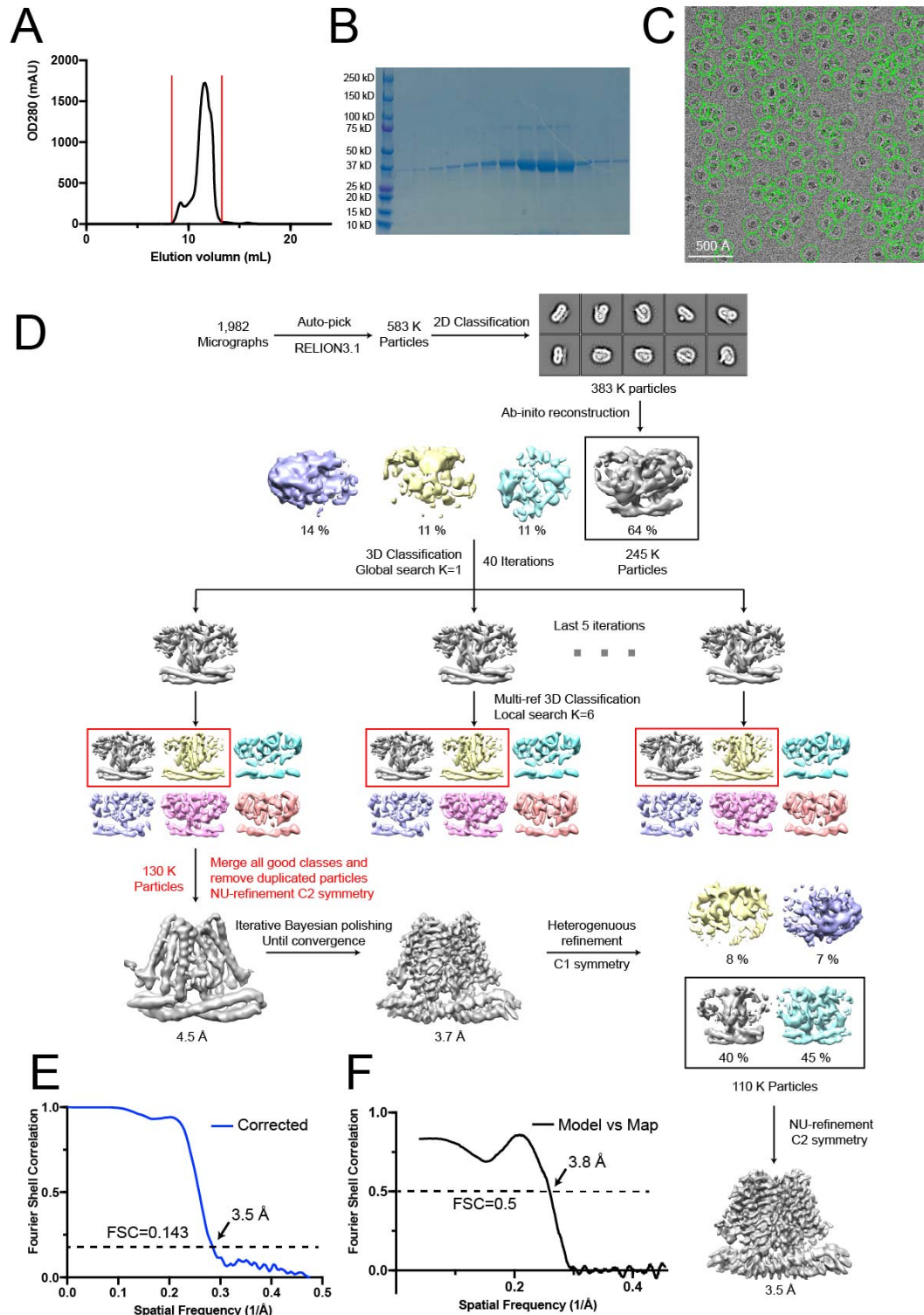


Figure 3 - figure supplement 1. Cryo-EM analysis of wild-type TACAN.

(A) Size-exclusion chromatography of TACAN on a Superdex 200 Increase 10/300 GL column.

(B) SDS- PAGE of fractions from size-exclusion chromatography between the red vertical lines shown in (A).

(C) Representative cryo-EM image of the TACAN^{WT}, selected particles are circled in green and the scale-bar is 50 nm.

(D) Cryo-EM data processing workflow for TACAN^{WT}.

(E) Gold-standard Fourier shell correlation (FSC) curve after correction for masking effects. The resolution was estimated based on the FSC = 0.143 criterion.

(F) FSC curve of the refined model versus EM map. The resolution was estimated based on the FSC = 0.5 criterion.

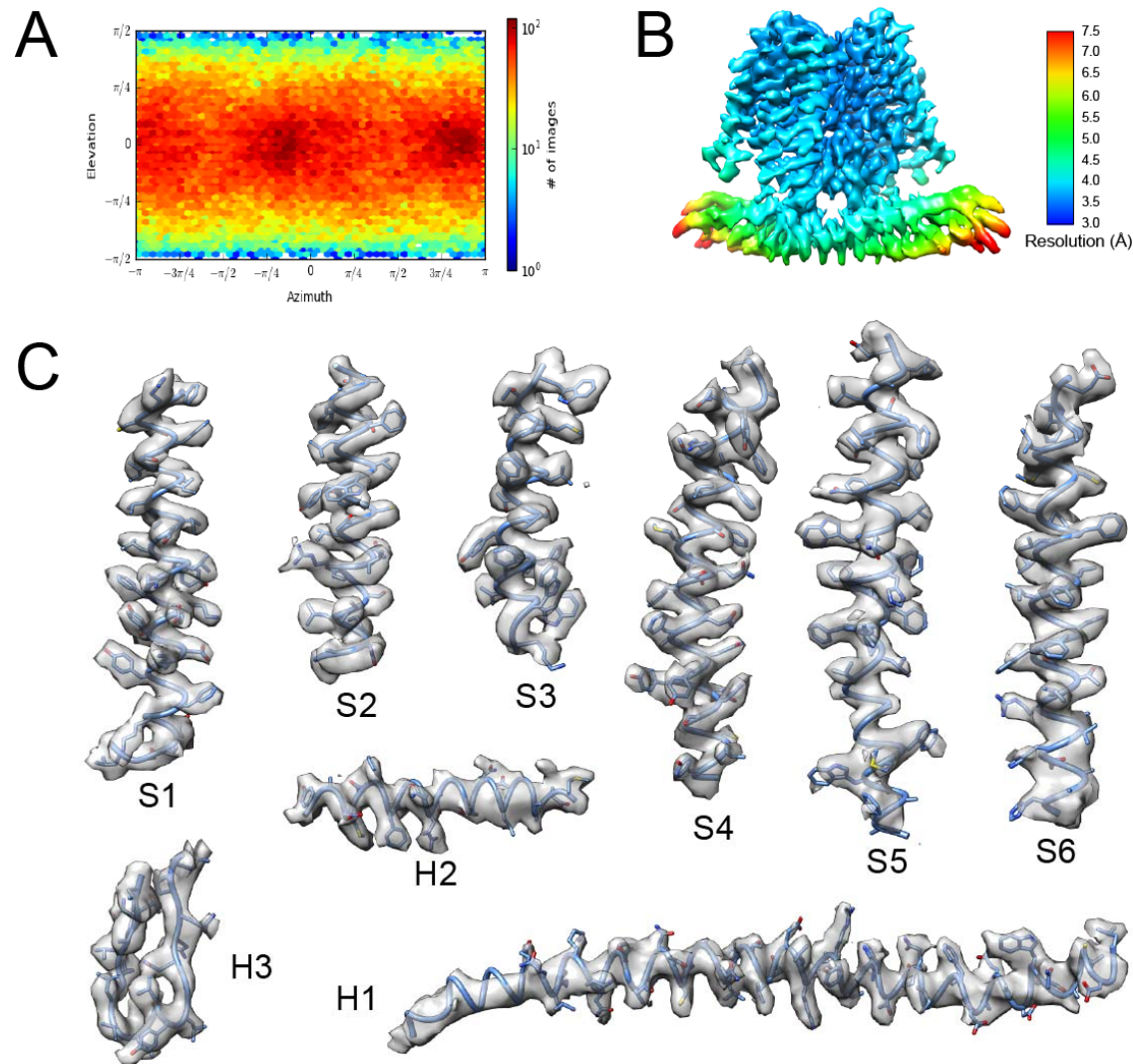


Figure 3 - figure supplement 2. Representative density in the Cryo-EM map of wild-type TACAN.

(A) The angular distribution of final reconstruction.

(B) Local resolution map of TACAN^{WT}.

(C) Cryo-EM densities for selected regions of TACAN^{WT} (contour level 4.4 in Coot).

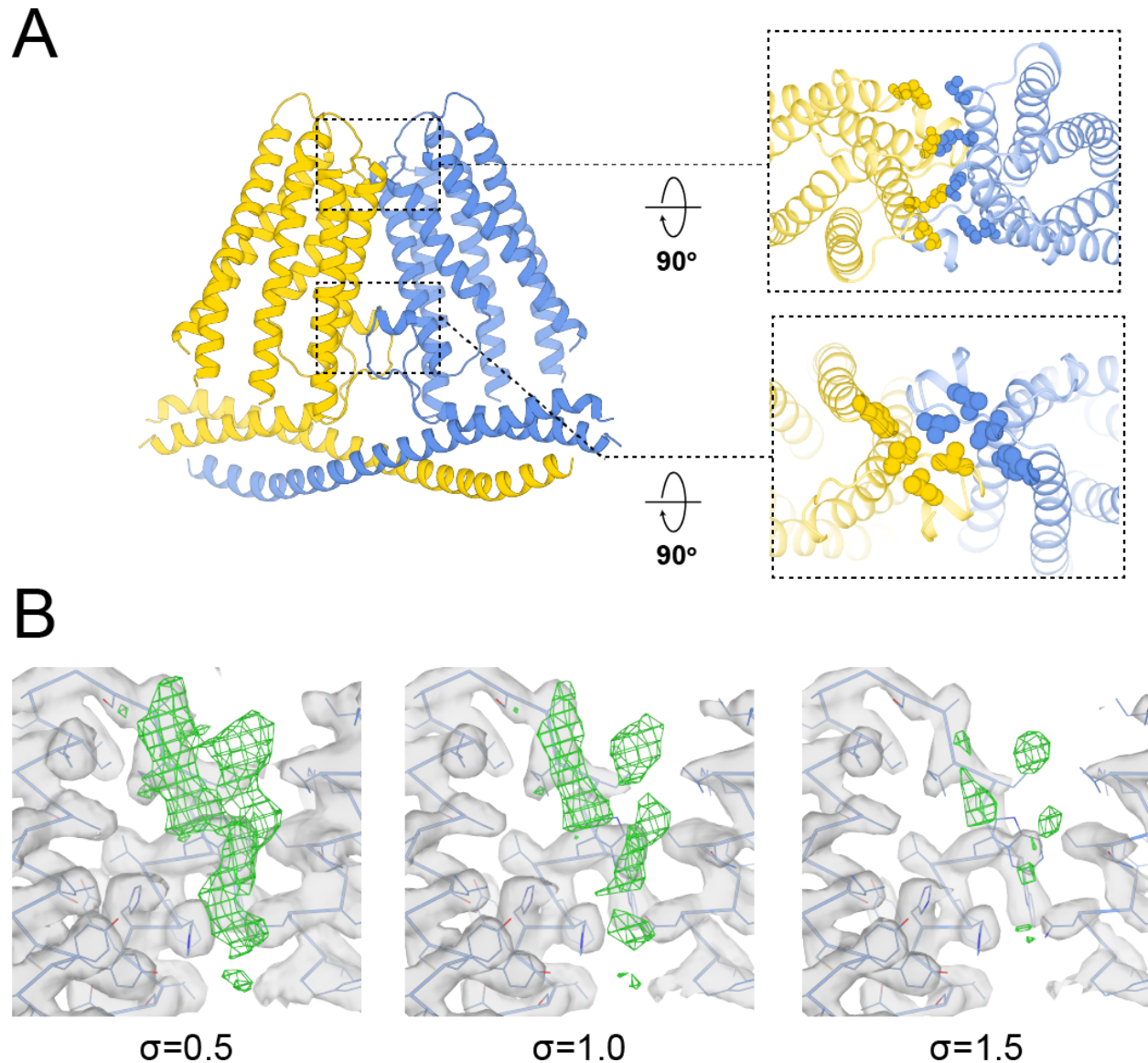


Figure 3 - figure supplement 3. Structural analysis of wild-type TACAN.

(A) Interactions of TACAN protomers at the dimer interface. The protomers are colored uniquely and the interfacial residues are shown in spheres.

(B) The non-protein density (green mesh) observed in TACAN^{WT} is shown at different contour levels (UCSF Chimera). The surrounding protein density is shown as gray surface.

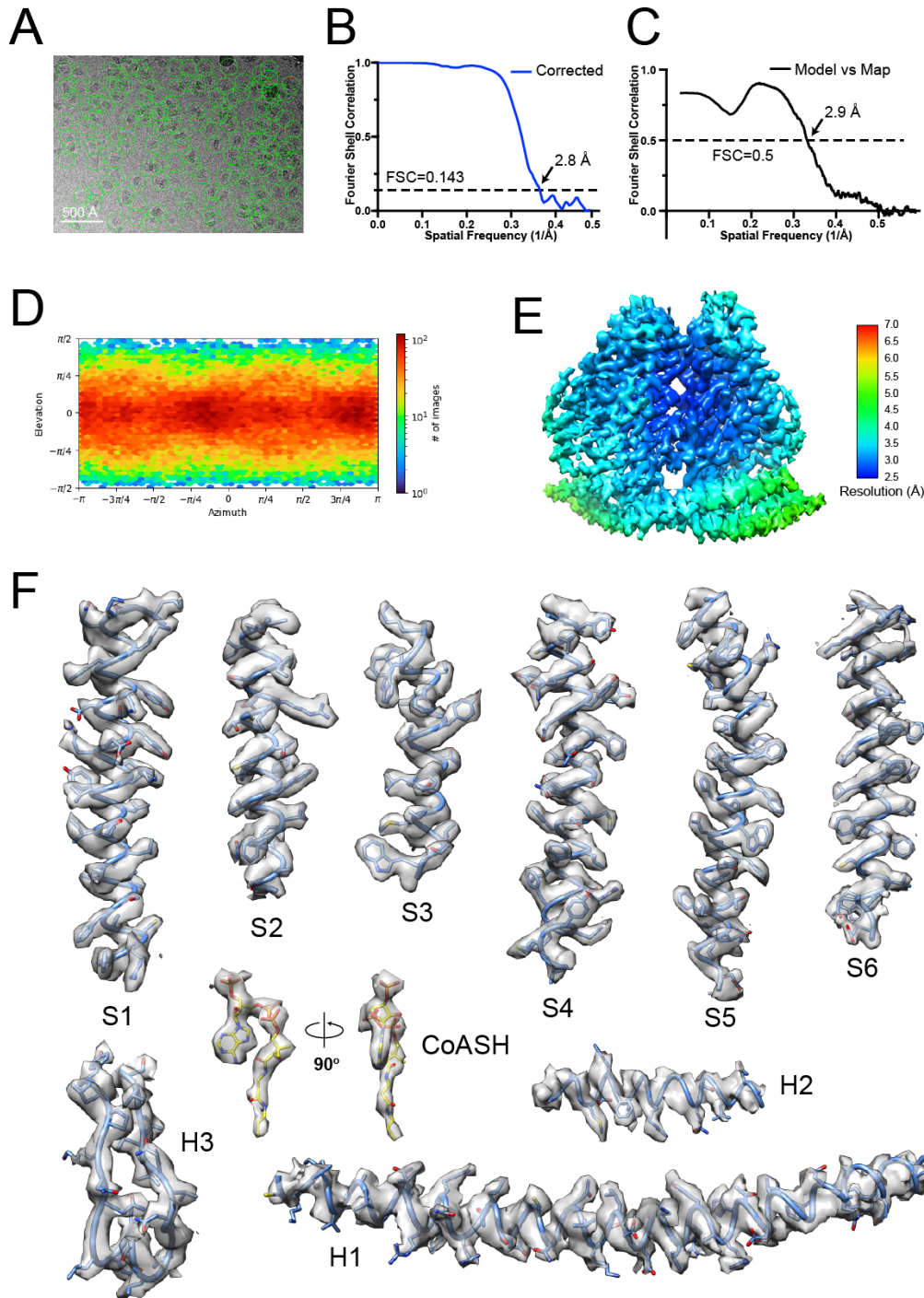


Figure 4 - figure supplement 1. Cryo-EM analysis of the His196Ala His197Ala mutant TACAN.

(A) Representative cryo-EM image of the TACAN^{H196A H197A}, selected particles are circled in green and the scale-bar is 50 nm.

(B) Gold-standard Fourier shell correlation (FSC) curve after correction for masking effects. The resolution was estimated based on the FSC = 0.143 criterion.

(C) FSC curve of the refined model versus EM map. The resolution was estimated based on the FSC = 0.5 criterion.

(D) The angular distribution of final reconstruction.

(E) Local resolution map of TACAN^{H196A H197A}.

(F) Cryo-EM densities for selected regions of TACAN^{H196A H197A} (contour level 5.2 in Coot). The CoASH molecule is colored according to atom type.

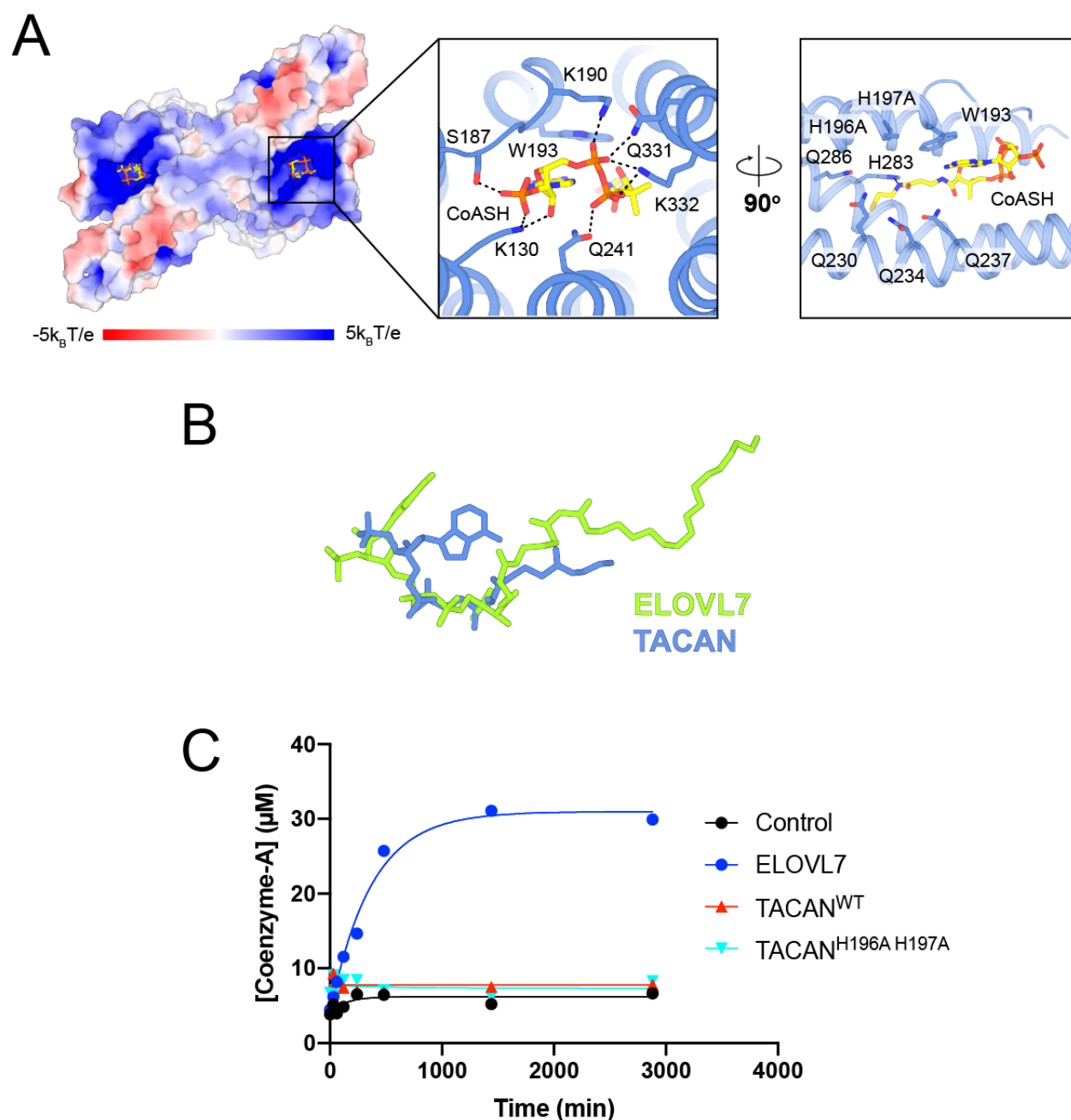


Figure 5 - figure supplement 1. TACAN is co-purified with coenzyme A molecules.

(A) Binding details of CoASH in TACAN^{H196A H197A}. Surface charge is represented from blue (positive charges) to red (negative charges). Neighboring residues are shown as sticks and the hydrogen bonding is indicated by a black dash. A CoASH molecule is shown as sticks and colored according to atom type.

(B) Conformation comparison of eicosanol-CoA in ELOVL7 (green) and CoASH in TACAN (blue) based on the alignment in Figure 4A.

(C) CoASH releasing activity of ELOVL7 and TACAN. Proteoliposomes of TACAN and ELOVL7 reconstituted in soy L- α -phosphatidylcholine (soy-PC) at 1:50 protein-to-lipid ratio (w/w) with 10 μ g protein and 500 μ g soy-PC were used. Empty proteoliposomes made of soy-PC were used as control. ELOVL7 showed significant activity, while neither the wild-type nor His196Ala His197Ala mutant of TACAN showed any activity.